Ab initio study of the structural, vibrational, and optical properties of potential parent structures of nitrogen-doped lutetium hydride

Đorđe Dangić [1,2,*] Peio Garcia-Goiricelaya [2] Yue-Wen Fang [1,2] Julen Ibañez-Azpiroz [2,3] and Ion Errea [1,2,4]

[1]*Fisika Aplikatua Saila, Gipuzkoako Ingeniaritza Eskola, University of the Basque Country (UPV/EHU), Europa Plaza 1, 20018 Donostia/San Sebastián, Spain*

[2]*Centro de Física de Materiales (CSIC-UPV/EHU), Manuel de Lardizabal Pasealekua 5, 20018 Donostia/San Sebastián, Spain*

[3]*IKERBASQUE Basque Foundation for Science, 48013 Bilbao, Spain*

[4]*Donostia International Physics Center (DIPC), Manuel de Lardizabal Pasealekua 4, 20018 Donostia/San Sebastián, Spain*

The recent report of near-ambient conditions superconductivity in a nitrogen-doped lutetium hydride has inspired a large number of experimental studies with contradictory results. We model from first principles the physical properties of the possible parent structures of the reported superconductors, LuH_2 and LuH_3. We show that only the phonon band structure of LuH_3 can explain the reported Raman spectra due to the presence of hydrogens at the interstitial octahedral sites. However, this structure is stabilized by anharmonicity only above 6 GPa. We find that the intriguing color change with pressure in the reported superconductor is consistent with the optical properties of LuH_2, which are determined by the presence of an undamped interband plasmon. The plasmon blueshifts with pressure and modifies the color of the sample without requiring any structural phase transition. Our findings suggest that the main component in the experiments is LuH_2 with some extra hydrogen atoms at octahedral sites. Neither LuH_2 nor LuH_3 superconducts at high temperatures.

I. INTRODUCTION

One of the most important problems of modern physics is finding a superconductor with a high critical temperature [1]. In the last ten years, high-pressure hydrides have emerged as promising candidates to achieve this goal [2,3]. After the initial confirmation of high-temperature superconductivity in H_3S at 140 GPa [4], a large number of different materials have been found to superconduct above liquid-nitrogen temperature [5–9]. However, all of these materials are only stable at high pressures and thus not technologically relevant. This instigated a secondary goal, finding a superconducting hydride at a near-ambient pressure.

Dasenbrock-Gammon *et al.* have recently reported a near-ambient pressure room-temperature superconductor in a nitrogen-doped lutetium hydride [10]. On the basis of Raman scattering, x-ray diffraction (XRD), and energy-dispersive x-ray experiments, the material has been identified with the $Fm\bar{3}m$ space group and the $LuH_{3-\delta}N_\epsilon$ stoichiometry, where the possibility of both N substitution (with concentration of ϵ per Lu atom) and H-vacancy defects (with concentration of δ per Lu atom) are remarked. The material has been reported to have a maximum superconducting critical temperature of 294 K at 1 GPa, accompanied by abrupt changes in the magnetic susceptibility, heat capacity, and resistance of the material. The paper reports as well an unexpected change in the color of the material with increasing pressure from blue to pink at 0.3 GPa, and finally to red at 3 GPa. The color change

is assigned to a phase transition. Finally, the Raman spectra reveal prominent phonon modes at three clearly separated energy ranges: below 150 cm^{-1}, around 250 cm^{-1}, and around 1200 cm^{-1}.

This finding has inspired a large number of experimental and theoretical works [11–18]. Unfortunately, none of these works has been able to reproduce the high-temperature superconductivity. Additionally, while qualitatively agreeing, most experiments quantitatively differ from each other. Firstly, the work in Ref. [14] reports the same sequence of colors of the material under pressure as in Ref. [10], but in pure LuH_2. However, the pressures at which the color of the sample changes are different, as well as for different samples investigated, implying a large inhomogeneity of the samples. The color change has been reported in a number of different works as well [14–16], all with similar color sequences and different transition pressures. Similar Raman spectra to that in Ref. [10] have been observed in other experiments and have been attributed both to LuH_2 [14,17] and to LuH_3 [18], where both octahedral and tetrahedral interstitial sites are occupied by hydrogen. The difficulty to correctly characterize these materials is expected since both LuH_2 and LuH_3 should have similar lattice constants and consequently XRD patterns.

In this study, we give an explanation for these experimental results by combining density functional theory (DFT) [19–27] with the stochastic self-consistent harmonic approximation (SSCHA) [28–32] to study structural, vibrational, optical, and superconducting properties of both LuH_2 and LuH_3. First, we report the structural and elastic properties of lutetium hydrides, which we find in reasonable agreement with experiments. The cubic LuH_3 shows imaginary phonon modes

*dorde.dangic@ehu.es

at 0 GPa and 0 K, even considering quantum anharmonic effects within the SSCHA. However, increasing pressure to 6 GPa and temperature to 300 K leads to a dynamically stable structure. We find that the 250-cm^{-1} phonon peak observed in Raman spectra could be a feature of the occupation of octahedral sites in LuH$_3$, only if quantum anharmonic effects are included. We have also calculated the optical reflectivity of both LuH$_2$ and LuH$_3$, and we only find the color change in LuH$_2$. LuH$_2$ has an undamped plasmon in the near-infrared region which gets blueshifted towards the visible spectrum with increasing pressure, leading to a color change. Considering the differences between experiments and calculations, our work suggests that the parent structure of the material in Ref. [10], as well as the materials observed in other experiments, is LuH$_2$ with slight doping of extra hydrogens in octahedral interstitial sites.

II. STRUCTURAL PROPERTIES AND PHONON DISPERSION

LuH$_2$ crystallizes in the cubic $Fm\bar{3}m$ structure, where Lu atoms form an fcc lattice and hydrogen atoms occupy tetrahedral sites. Experiments report a lattice constant of 5.033 Å [33] at 300 K or 5.028 Å [34] at 100 K. We have relaxed the structure of LuH$_2$ in static DFT, neglecting the zero-point energy, and within the SSCHA to account for it as well as anharmonicity. At 0 K we obtain the value of 5.07 Å within the SSCHA, which is a slight overestimation, expected for the generalized gradient approximation exchange-correlation functional used. At ambient pressure LuH$_3$ crystallizes in the $P\bar{3}c1$ phase [18,35]. With increasing pressure, it transforms to a cubic $Fm\bar{3}m$ structure, which is identical to LuH$_2$ with an additional hydrogen at the octahedral site. Experimentally, the phase transition between $P\bar{3}c1$ and $Fm\bar{3}m$ is reported at 12 GPa [36] or 2 GPa [18]. Our static DFT simulations predict the phase transition at 25 GPa (see Supplemental Material [37]). The disagreement between experiment and theory could be reconciled by accounting for anharmonic and zero-point motion effects within SSCHA. Due to the high computational cost for the less-symmetric $P\bar{3}c1$ phase, we have not performed these calculations. An additional reason for the discrepancy between calculations and experiments, as well as between different experiments, could be the existence of hydrogen vacancies in LuH$_3$ samples.

We have calculated the bulk modulus for cubic LuH$_2$ and LuH$_3$ by fitting the static DFT energy to a third-order polynomial. Our results for LuH$_2$ give a bulk modulus of $B = 90.6$ GPa, and bulk modulus pressure derivative of $K_0 = 4.6$, which agree fairly well with the values found in Ref. [10] ($B = 88.6$ GPa and $K_0 = 4$). The reported experimental value for LuH$_3$, $B = 89$ GPa [38], is very close to the value reported in Ref. [10]. The DFT results for cubic LuH$_3$ give a decent agreement for bulk modulus pressure derivative $K_0 = 4$, but overestimate the value for bulk modulus $B = 104.7$ GPa. However, including anharmonic and quantum effects is going to lower the value of the bulk modulus, leading to a better agreement with the experiment for LuH$_3$. The literature also reports thermal expansion coefficients for LuH$_2$, 1.1985×10^{-5} 1/K [34] and 3.55×10^{-5} 1/K [33]. Within the SSCHA
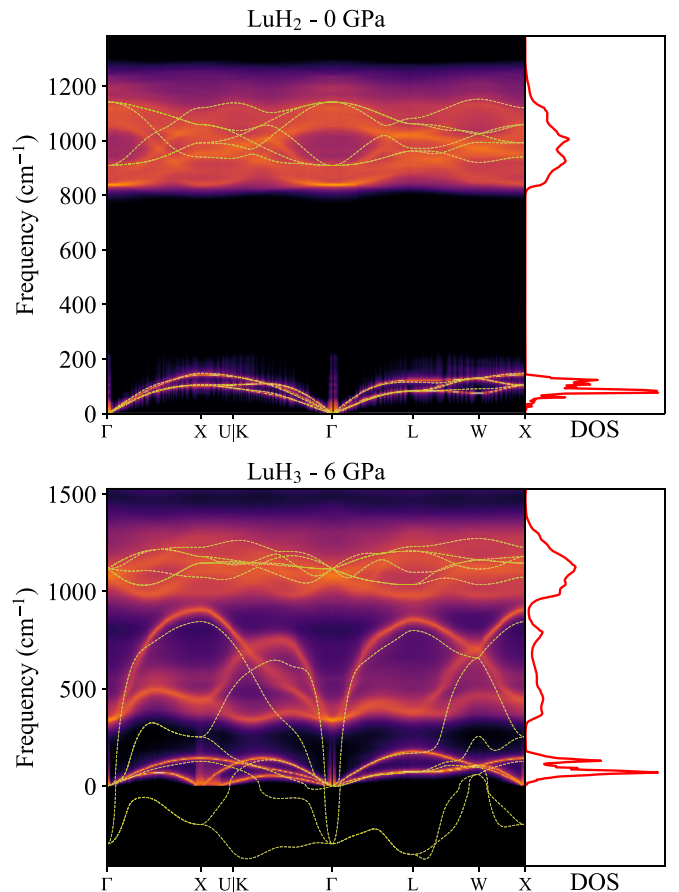

FIG. 1. Phonon spectral function of LuH$_2$ (0 GPa) and LuH$_3$ (6 GPa) at 300 K. Side figures are showing phonon density of states obtained as a sum of the phonon spectral functions. The dashed lines are phonon frequencies calculated from DFPT (harmonic) force constants.

the volume thermal expansion coefficient is 2.77×10^{-5} 1/K, in good agreement with experiments.

We calculate the phonon properties of lutetium hydrides at the harmonic level within density functional perturbation theory (DFPT) [25–27] and including anharmonicity within the SSCHA (see Fig. 1). LuH$_2$ is very harmonic and both harmonic DFPT and SSCHA calculations give similar phonon band structures. Including dynamical effects through the dynamical bubble approximation [39] leads to moderate phonon spectral broadening and small temperature line shifts. In LuH$_2$ phonon modes are separated into two groups: low-frequency modes (below 200 cm^{-1}), which have mostly lutetium character, and high-frequency (around 1000 cm^{-1}) optical modes associated to hydrogen atoms in the tetrahedral sites. These bands are separated with a large frequency gap and cannot explain the Raman spectra in lutetium hydrides, which show phonon modes inside this gap [10,17,18].

Cubic LuH$_3$ is dynamically unstable at 0 GPa [11], showing imaginary phonon frequencies throughout the Brillouin zone. If we apply pressure of 6 GPa and increase the temperature to 300 K the structure stabilizes due to anharmonicity, as evidenced by the SSCHA free-energy Hessian dispersion (see Supplemental Material [37]). This compound is therefore

strongly anharmonic, as it happens for other fcc metals with H atoms in octahedral sites [29,30,40]. The spectral function calculation reveals there might be an instability around the X point of the Brillouin zone. A closer inspection of the spectral function at this point reveals strong softening. However, the spectral weight goes to zero as ω goes to zero and thus it is not an instability. Phonons of this phase strongly resemble those of LuH_2 with additional phonon branches inside the acoustic-optical frequency gap. These phonons are associated with hydrogen atoms in octahedral sites and are not Raman active. However, if there is enough disorder in the experimental sample, they could be the source of the $250\,\mathrm{cm^{-1}}$ peak. In our calculations, octahedral site modes are very sensitive to the applied pressure, considerably more than in the experiment [15]. They stiffen above $300\,\mathrm{cm^{-1}}$ at 6 GPa and thus cannot be conclusively identified as the origin of the $250\,\mathrm{cm^{-1}}$ peak. On the other hand, the octahedral modes are not at all present in LuH_2 and thus are a strong indication that we have at least partial occupation of octahedral sites in the samples. Alternatively, the Raman signal at $250\,\mathrm{cm^{-1}}$ from Ref. [10] could be explained by nitrogen-dominated modes, which should exist in this frequency range. However, this does not explain why these modes are also observed in undoped LuH_2 and LuH_3 samples [14,17,18].

III. OPTICAL PROPERTIES

The color change of the sample in the experiment in Ref. [10] is very intriguing. It has been reproduced multiple times in different experiments but with different transition pressures for the color changes [14,15]. To model this behavior of lutetium hydrides, we performed electronic band structure calculations and, afterward, calculated the optical dielectric function within the random-phase approximation by means of Wannier interpolation. From the dielectric function, it is straightforward to obtain the reflectivity of the sample using the Fresnel equation. The actual color of the sample is calculated by converting the reflectivity using color-matching functions to a standard RGB format [41]. The results are presented in Fig. 2. The color of LuH_2 is changing from blue to red in the span of 26 GPa, which is in agreement with one of the experiments [15]. Since in the experiment the sample is loaded in the diamond-anvil cell, in the Fresnel equations we assume that the light reflects from the diamond. This is probably the source of disagreement between our calculations and some of the recent ones [13], where the medium is assumed to be a vacuum, which resulted in color transitions at much higher pressures. On the other hand, the cubic LuH_3 does not show any color change in the considered pressure range.

The reason for the color change in LuH_2 is the existence of an undamped interband plasmon [42] in the near-infrared region and a lack of interband electronic optical transitions below 2 eV (see Supplemental Material [37]). The onset of interband transitions makes the imaginary part of the dielectric function soar from zero to above approximately 2 eV, making the real part cross the zero value at lower energies due to Kramers-Kronig relations. Thus, both real and imaginary parts of the dielectric function are zero at the same energy and the energy-loss function has a Dirac delta peak at this energy, resulting in an undamped plasmon peak (see Fig. 3).
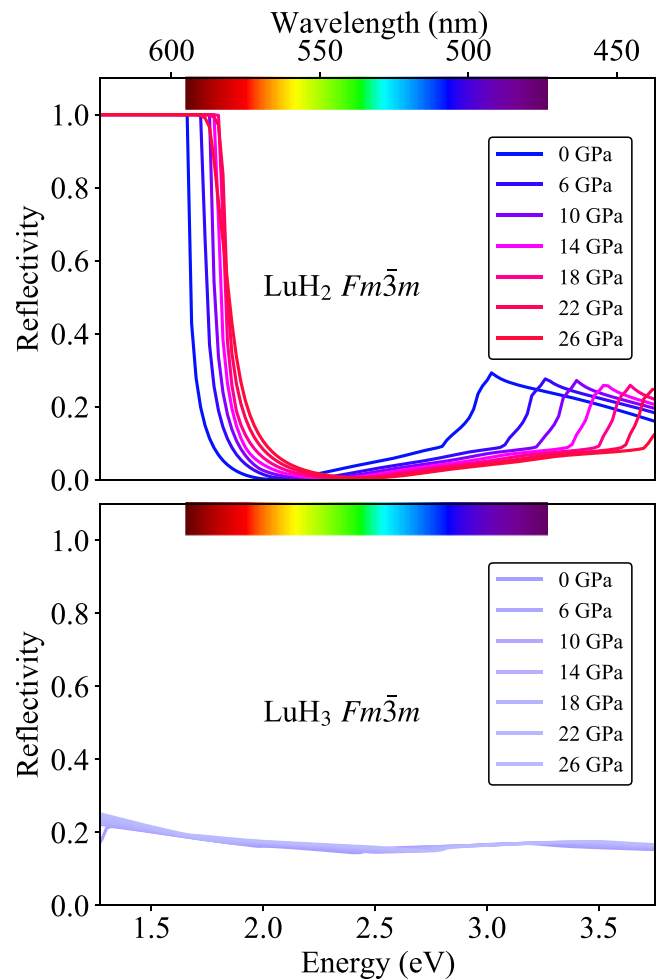

FIG. 2. Calculated reflectivities of LuH_2 (top panel) and LuH_3 (bottom panel). The line color represents the perceived color calculated from the reflectivity data.

The presence of the plasmon is responsible for suppressing the large reflectivity in the far infrared, consequently making the sample blue. As pressure is increased, this plasmon blueshifts and the highly reflecting region enters the visible range, making the overall color of the sample red and shiny. Interband transitions are present at all energies in LuH_3 and hence it does not have any interband plasmon in the optical range. Its optical properties barely change with pressure and there is no color change. Additionally, LuH_3 samples should reflect much less light than LuH_2.

In the study we are not including the effects of electron-phonon coupling on optical properties of LuH_2 and LuH_3. In LuH_2, electron-phonon interaction will lead to the broadening of the electronic band structure in Fig. 3 and push the onset of available interband transition to slightly lower energies. This will not lead to a large change in reflectivity and the color change should happen at similar pressures. In LuH_3 the effect of electron-phonon coupling should be even smaller due to the fact that electronic interband transitions are already allowed.

IV. DISCUSSION

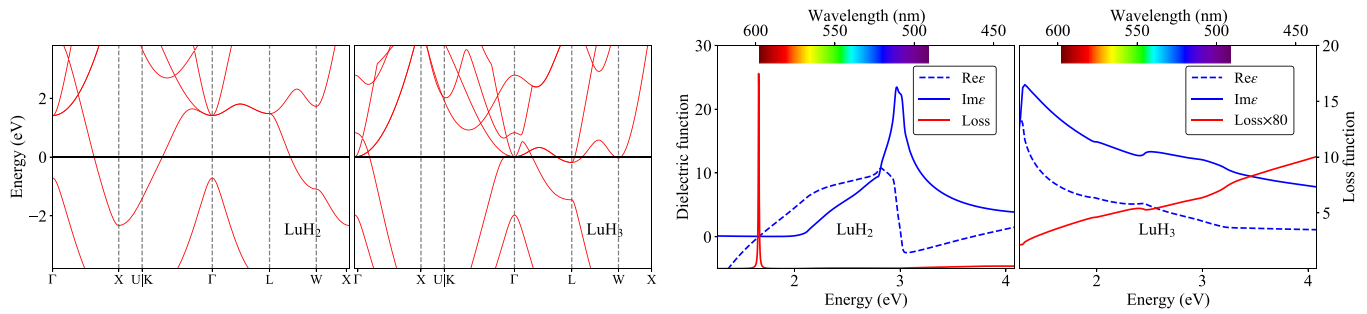At this moment, we have contradictory findings. While the Raman signal can only be explained by LuH_3, the color

FIG. 3. Electronic band structure of LuH_2 and LuH_3 at 0 GPa. The real and imaginary parts of the dielectric function $\varepsilon(\omega)$ calculated in the random-phase approximation are given as dashed and full blue lines, respectively. The energy-loss function, $-Im[\varepsilon(\omega)^{-1}]$, is given as a full red line.

changes induced by pressure only exist in LuH_2. As we mentioned before, XRD cannot distinguish between these two materials, while the calculated lattice constant is overestimated in DFT/SSCHA for both of the models. The calculated elastic constants are similar enough that we cannot say with certainty which material appears in the experiments. Some previous experiments suggested that the stoichiometry of lutetium hydride is between lutetium dihydride and lutetium trihydride [43]. Indeed, at 1 GPa doping the lutetium dihydride with H (Lu_4H_9) puts it only 12 meV/atom above the convex hull, which is significantly lower than LuH_3 (82 meV/atom). The crystal structure search that we have performed (see Supplemental Material) with Lu_4H_9 stoichiometry suggests that extra H should go into the octahedral sites. This configuration will give rise to the octahedral site optical phonon modes that are the best candidate for the source of the Raman peak at 250 cm^{-1} in experiments. However, this addition also pushes the plasmon deeper into the infrared region, which means that the color change would be induced at higher pressures than in pure LuH_2.

We have also considered the case of LuH_2 with vacancies on the tetrahedral site. Our crystal structure predictions reveal that in this case (Lu_4H_7), the energy above the convex hull is slightly higher compared to hydrogen-doped LuH_2 (Lu_4H_9), specifically by 27 meV as opposed to 12 meV. The Lu_2H_3 structure is red already at 0 GPa and with increasing pressure changes color to yellow/orange. Additionally, it is not able to explain the 250-cm^{-1} Raman peak since it does not have phonon modes in the acoustic-optical phonon gap.

Finally, we have also calculated the superconducting properties of lutetium dihydride and trihydride using isotropic Migdal-Eliashberg equations. In agreement with experiments [43,44] and recent theoretical work [11,13] we do not find superconductivity in LuH_2. Using the stable structure of LuH_3 at 6 GPa and 300 K, we find that LuH_3 should have a critical temperature of 19 K, which is well below the temperature needed to stabilize it. We find that the anharmonicity of

phonon modes plays a large role in determining the critical temperature, as it changes by 50% depending on the method used to calculate the Eliashberg spectral function $\alpha^2F(\omega)$. The modes that contribute significantly to $\alpha^2F(\omega)$ are the octahedral modes, as happens in palladium hydrides [40], which explains the existence of superconductivity in LuH_3 and not in LuH_2.

In conclusion, we have performed a first-principles study of the physical properties of lutetium hydrides in order to recognize the parent structure of the material synthesized in Ref. [10]. We find that both LuH_2 and LuH_3 have similar structural and elastic properties and are thus indistinguishable in XRD experiments. Their phonon band structures, however, are considerably different, with only LuH_3 being able to explain experimental findings. LuH_3 is dynamically unstable at 0 K and 0 GPa but stabilizes at pressures above 6 GPa above room temperature thanks to anharmonic effects. The color change observed in many experiments is only a feature of LuH_2 and does not take place in LuH_3. For these reasons, we believe that the structure which is synthesized in most experiments is LuH_2 with extra hydrogens in octahedral sites. Isotropic Migdal-Eliashberg calculations show that LuH_2 is not a superconductor, while LuH_3 has a modest critical temperature, significantly less than what is reported in Ref. [10].

[1] V. L. Ginzburg, Phys. Usp. **42**, 353 (1999).

[2] C. J. Pickard, I. Errea, and M. I. Eremets, Annu. Rev. Condens. Matter Phys. **11**, 57 (2020).

[3] B. Lilia, R. Hennig, P. Hirschfeld, G. Profeta, A. Sanna, E. Zurek, W. E. Pickett, M. Amsler, R. Dias, M. I. Eremets, C. Heil, R. J. Hemley, H. Liu, Y. Ma, C. Pierleoni, A. N. Kolmogorov, N. Rybin, D. Novoselov, V. Anisimov, A. R. Oganov *et al.*, J. Phys.: Condens. Matter **34**, 183002 (2022).

[4] A. P. Drozdov, M. I. Eremets, I. A. Troyan, V. Ksenofontov, and S. I. Shylin, Nature (London) **525**, 73 (2015).

[5] M. Somayazulu, M. Ahart, A. K. Mishra, Z. M. Geballe, M. Baldini, Y. Meng, V. V. Struzhkin, and R. J. Hemley, Phys. Rev. Lett. **122**, 027001 (2019).

[6] A. P. Drozdov, P. P. Kong, V. S. Minkov, S. P. Besedin, M. A. Kuzovnikov, S. Mozaffari, L. Balicas, F. F. Balakirev, D. E. Graf, V. B. Prakapenka, E. Greenberg, D. A. Knyazev, M. Tkacz, and M. I. Eremets, Nature (London) **569**, 528 (2019).

[7] I. A. Troyan, D. V. Semenok, A. G. Kvashnin, A. V. Sadakov, O. A. Sobolevskiy, V. M. Pudalov, A. G. Ivanova, V. B. Prakapenka, E. Greenberg, A. G. Gavriliuk, I. S. Lyubutin, V. V. Struzhkin, A. Bergara, I. Errea, R. Bianco, M. Calandra, F. Mauri, L. Monacelli, R. Akashi, and A. R. Oganov, Adv. Mater. **33**, 2006832 (2021).

[8] P. Kong, V. S. Minkov, M. A. Kuzovnikov, A. P. Drozdov, S. P. Besedin, S. Mozaffari, L. Balicas, F. F. Balakirev, V. B. Prakapenka, S. Chariton, D. A. Knyazev, E. Greenberg, and M. I. Eremets, Nat. Commun. **12**, 5075 (2021).

[9] L. Ma, K. Wang, Y. Xie, X. Yang, Y. Wang, M. Zhou, H. Liu, X. Yu, Y. Zhao, H. Wang, G. Liu, and Y. Ma, Phys. Rev. Lett. **128**, 167001 (2022).

[10] N. Dasenbrock-Gammon, E. Snider, R. McBride, H. Pasan, D. Durkee, N. Khalvashi-Sutter, S. Munasinghe, S. E. Dissanayake, K. V. Lawler, A. Salamat, and R. P. Dias, Nature (London) **615**, 244 (2023).

[11] R. Lucrezi, P. P. Ferreira, M. Aichhorn, and C. Heil, arXiv:2304.06685.

[12] X. Tao, A. Yang, S. Yang, Y. Quan, and P. Zhang, Sci. Bull. **68**, 1372 (2023).

[13] S.-W. Kim, L. J. Conway, C. J. Pickard, G. L. Pascut, and B. Monserrat, arXiv:2304.07326.

[14] P. Shan, N. Wang, X. Zheng, Q. Qiu, Y. Peng, and J. Cheng, Chin. Phys. Lett. **40**, 046101 (2023).

[15] X. Xing, C. Wang, L. Yu, J. Xu, C. Zhang, M. Zhang, S. Huang, X. Zhang, B. Yang, X. Chen, Y. Zhang, J.-g. Guo, Z. Shi, Y. Ma, C. Chen, and X. Liu, arXiv:2303.17587.

[16] Y.-J. Zhang, X. Ming, Q. Li, X. Zhu, B. Zheng, Y. Liu, C. He, H. Yang, and H.-H. Wen, Sci. China Phys. Mech. Astron. **66**, 287411 (2023).

[17] P. Li, J. Bi, S. Zhang, R. Cai, G. Su, F. Qi, R. Zhang, Z. Wei, and Y. Cao, Chin. Phys. Lett. **40**, 087401 (2023).

[18] O. Moulding, S. Gallego-Parra, Y. Gao, P. Toulemonde, G. Garbarino, P. De Rango, S. Pairis, P. Giroux, M.-A. Méasson, arXiv:2304.04310.

[19] J. P. Perdew, K. Burke, and M. Ernzerhof, Phys. Rev. Lett. **77**, 3865 (1996).

[20] S. L. Dudarev, G. A. Botton, S. Y. Savrasov, C. J. Humphreys, and A. P. Sutton, Phys. Rev. B **57**, 1505 (1998).

[21] M. van Setten, M. Giantomassi, E. Bousquet, M. Verstraete, D. Hamann, X. Gonze, and G.-M. Rignanese, Comput. Phys. Commun. **226**, 39 (2018).

[22] P. Giannozzi, S. Baroni, N. Bonini, M. Calandra, R. Car, C. Cavazzoni, D. Ceresoli, G. L. Chiarotti, M. Cococcioni, I. Dabo, A. D. Corso, S. de Gironcoli, S. Fabris, G. Fratesi, R. Gebauer, U. Gerstmann, C. Gougoussis, A. Kokalj, M. Lazzeri, L. Martin-Samos *et al.*, J. Phys.: Condens. Matter **21**, 395502 (2009).

[23] P. Giannozzi, O. Andreussi, T. Brumme, O. Bunau, M. B. Nardelli, M. Calandra, R. Car, C. Cavazzoni, D. Ceresoli, M. Cococcioni, N. Colonna, I. Carnimeo, A. D. Corso, S. de Gironcoli, P. Delugas, R. A. DiStasio, A. Ferretti, A. Floris, G.

Fratesi, G. Fugallo *et al.*, J. Phys.: Condens. Matter **29**, 465901 (2017).

[24] P. Giannozzi, O. Baseggio, P. Bonfá, D. Brunato, R. Car, I. Carnimeo, C. Cavazzoni, S. de Gironcoli, P. Delugas, F. Ferrari Ruffino, A. Ferretti, N. Marzari, I. Timrov, A. Urru, and S. Baroni, J. Chem. Phys. **152**, 154105 (2020).

[25] S. Baroni, S. de Gironcoli, A. Dal Corso, and P. Giannozzi, Rev. Mod. Phys. **73**, 515 (2001).

[26] A. Floris, I. Timrov, B. Himmetoglu, N. Marzari, S. de Gironcoli, and M. Cococcioni, Phys. Rev. B **101**, 064305 (2020).

[27] A. Floris, S. de Gironcoli, E. K. U. Gross, and M. Cococcioni, Phys. Rev. B **84**, 161102(R) (2011).

[28] L. Monacelli, R. Bianco, M. Cherubini, M. Calandra, I. Errea, and F. Mauri, J. Phys.: Condens. Matter **33**, 363001 (2021).

[29] I. Errea, M. Calandra, and F. Mauri, Phys. Rev. Lett. **111**, 177002 (2013).

[30] I. Errea, M. Calandra, and F. Mauri, Phys. Rev. B **89**, 064302 (2014).

[31] R. Bianco, I. Errea, L. Paulatto, M. Calandra, and F. Mauri, Phys. Rev. B **96**, 014111 (2017).

[32] L. Monacelli, I. Errea, M. Calandra, and F. Mauri, Phys. Rev. B **98**, 024106 (2018).

[33] J. E. Bonnet and J. N. Daou, J. Appl. Phys. **48**, 964 (1977).

[34] N. Wang, J. Hou, Z. Liu, P. Shan, C. Chai, S. Jin, X. Wang, Y. Long, Y. Liu, H. Zhang, X. Dong, and J. Cheng, arXiv:2304.00558.

[35] M Mansmann and W. E. Wallace, J. Phys. (Paris) **25**, 454 (1964).

[36] M. Tkacz and T. Palasyuk, J. Alloys Compd. **446-447**, 593 (2007).

[37] See Supplemental Material at http://link.aps.org/supplemental/10.1103/PhysRevB.108.064517 for more details on the calculations, the phonons, elastic and structural properties of LuH$_2$ and LuH$_3$, and superconducting properties of LuH$_3$, which includes Refs. [45–55].

[38] T. Palasyuk and M. Tkacz, Solid State Commun. **133**, 481 (2005).

[39] L. Monacelli and F. Mauri, Phys. Rev. B **103**, 104305 (2021).

[40] A. Meninno and I. Errea, Phys. Rev. B **107**, 024504 (2023).

[41] G. Prandini, G.-M. Rignanese, and N. Marzari, npj Comput. Mater. **5**, 129 (2019).

[42] I. Errea, A. Rodriguez-Prieto, B. Rousseau, V. M. Silkin, and A. Bergara, Phys. Rev. B **81**, 205105 (2010).

[43] J. N. Daou, P. Vajda, J. P. Burger, and D. Shaltiel, Europhys. Lett. **6**, 647 (1988).

[44] J. N. Daou, A. Lucasson, P. Vajda, and J. P. Burger, J. Phys. F **14**, 2983 (1984).

[45] Đ. Dangić, L. Monacelli, R. Bianco, F. Mauri, and I. Errea, arXiv:2303.07962.

[46] G. Pizzi, V. Vitale, R. Arita, S. Blügel, F. Freimuth, G. Géranton, M. Gibertini, D. Gresch, C. Johnson, T. Koretsune, J. Ibañez-Azpiroz, H. Lee, J.-M. Lihm, D. Marchand, A. Marrazzo, Y. Mokrousov, J. I. Mustafa, Y. Nohara, Y. Nomura, L. Paulatto *et al.*, J. Phys.: Condens. Matter **32**, 165902 (2020).

[47] P. Garcia-Goiricelaya, J. Krishna, and J. Ibañez-Azpiroz, Phys. Rev. B **107**, 205101 (2023).

[48] J. R. Yates, X. Wang, D. Vanderbilt, and I. Souza, Phys. Rev. B **75**, 195121 (2007).

[49] X. Wang, J. R. Yates, I. Souza, and D. Vanderbilt, Phys. Rev. B **74**, 195118 (2006).

[50] G. Bellomia and R. Resta, Phys. Rev. B **102**, 205123 (2020).

[51] Y. Wang, J. Lv, L. Zhu, and Y. Ma, Phys. Rev. B **82**, 094116 (2010).

[52] Y. Wang, J. Lv, L. Zhu, and Y. Ma, Comput. Phys. Commun. **183**, 2063 (2012).

[53] G. Kresse and J. Furthmüller, Phys. Rev. B **54**, 11169 (1996).

[54] G. Kresse and J. Furthmüller, Comput. Mater. Sci. **6**, 15 (1996).

[55] A. Jain, G. Hautier, C. J. Moore, S. Ping Ong, C. C. Fischer, T. Mueller, K. A. Persson, and G. Ceder, Comput. Mater. Sci. **50**, 2295 (2011).